Operational Aspects of the 16 April Tornadoes and the 27-28 April 2011 Tornado Outbreak in the WFO LWX Forecast Area

Matthew R. Kramar, Steven Zubrick and James E. Lee
National Weather Service
Baltimore/Washington Weather Forecast Office
Sterling, VA

1. INTRODUCTION

April 2011 was an unusually prolific month for tornadoes across portions of the eastern half of the United States, with more than 450 tornadoes east of the Mississippi River officially recorded (to date) in the National Weather Service (NWS) *Storm Data* publication. The Baltimore/ Washington Forecast Office (WFO) in Sterling, VA (WFO LWX) experienced two significant tornadic episodes: one on 16 April; the other spanning 27-28 April 2011. Both episodes contributed to a near-record tornado season in the WFO LWX forecast area. During the 27-28 April tornado outbreak, portions of the WFO LWX forecast area were under a Tornado Watch for nearly 24 hours (an unprecedented length of time for this part of the country), with at least 19 tornadoes of EF-0 to EF-2 intensity during a 17-hour period.

The WFO LWX forecast area is unique owing to the presence of four Federal Aviation Administration (FAA) Terminal Doppler Weather Radars (TDWRs) in addition to the NWS WFO LWX Weather Surveillance Radar-88 Doppler (WSR-88D) in Sterling (note: the LWX-88D radar had not been upgraded to dual-polarization during the April 2011 episodes). The four TDWRs offer warning forecasters one-minute updates of low-level reflectivity and velocity data in addition to the four-minute volume scan updates provided by the WSR-88D. Owing to the comparatively higher temporal and spatial resolution of the TDWR data, low-level reflectivity and velocity features are detected and tracked far more readily than in WSR-88D data.

A cursory synoptic overview is given for each case, with a more detailed examination of radar data during the tornadic events of 16 April 2011. In particular, a dual-radar examination of a close-proximity mesocyclonic tornadic supercell embedded in a convective line on 16 April is offered in addition to depictions of cyclic non-mesocyclonic tornadogenesis in a quasi-linear convective system (QLCS). Impacts and implications of these data on subsequent storm surveys are discussed. Operational challenges faced by WFO LWX during the 27-28 April tornado outbreak in the Mid-Atlantic Region also are highlighted.

Corresponding author address:
Matthew R. Kramar
NWS WFO Baltimore/Washington
43858 Weather Service Road
Sterling, VA 20166

Email: matthew.kramar@noaa.gov

2. 16 APRIL 2011 TORNADOES

a. Synoptic overview

At 17 April 0000 UTC, a negatively-tilted trough was moving northeastward across the Great Lakes region at 500 hPa (Fig. 1, upper pane), and an associated jet maximum at 500 hPa was found over the Mid-Atlantic region. At the surface (not shown), low pressure was centered over Michigan while a negatively-tilted surface trough axis extended southeastward through Pennsylvania. A second low pressure center was organizing over Northern Virginia.

Owing to the strong southerly winds, a very moist boundary layer characterized by surface dewpoints in the lower 60s F was present east of the Blue Ridge Mountains, while temperatures in the mid 60s F were common. The 17 April 0000 UTC RAOB taken at KIAD (Fig. 1, lower panel) sampled the pre-storm environment, released just ahead of an approaching convective line. The environment was characterized by weak lapse rates and modest instability but very high shear. The hodograph exhibited a clockwise semicircular shape through 600 hPa and was unidirectional through the lowest 700m with the low-level environmental vorticity vector oriented westward. The shear was more than sufficient for organized updrafts. During the afternoon of the 16 April, a line of relatively shallow convection developed along the surface trough axis in the strongly-forced, weakly unstable environment.

b. Leesburg, VA supercell

A supercell developed in western Loudoun County Virginia, embedded in a line of convection along the surface trough axis. A mid-level mesocyclone formed in the cell's updraft along the leading edge of the line. This storm was sampled from close proximity by both KLWX (WSR-88D) and the nearby FAA/TDWR (TIAD) radars. At 2307 UTC (Fig. 2a), the mesocyclone had not descended through the lowest elevation slices of the radars, as evidenced by the linear structure to the low-level outflow boundary.

Through the next four minutes (Fig. 2b), a rear-flank downdraft developed and surged northeastward beneath the updraft as a low-level mesocyclone became organized. A hook echo developed concurrently along the forward flank of the storm in both TDWR and WSR-88D data.

Multiple rings of low reflectivity became evident at 2313 UTC (Fig. 2c) in TIAD data, highlighting the intensity of the circulation and the multiple scales of rotation. At this time,

the TIAD radar was located ~5 km from the mesocyclone precisely downstream of the storm, and sampled the storm at ~125m AGL, below cloud base, providing a relatively uncommon perspective of the tornadic-phase evolution. At this time (2313 UTC), the rear-flank downdraft was located beneath the low-level mesocyclone. At 2316 UTC (Fig. 2d), reflectivity began to fill the low-level circulation as the forward-flank and rear-flank downdrafts merged and undercut the circulation. Thereafter, the updraft lost its supercellular characteristics and became assimilated into the line of storms that progressed east-northeastward into Frederick and Carroll Counties.

A continuous path of damage mainly to trees and sign posts was documented from near Hughesville, VA to southern Leesburg, VA. A NOAA employee observed a funnel cloud as the circulation contracted and passed over his home near Hughesville (White 'X' in Fig. 2b, 2310 UTC). A 29 m/s wind gust was measured in the tornado's infancy in the outer portion of the circulation, where damage was sustained to shingles. An estimated gust to 31 m/s was provided by a trained storm spotter farther east along the tornado's path, where a wooden sign post was ripped from the ground and dragged several tens of meters downwind. All damage was consistent with an EF0 tornado along the ~6.5 km path.

c. Frederick and Carroll Counties, MD tornadoes

Later on 16 April 2011, an organized line of low-topped thunderstorms moved across Frederick and Carroll Counties in central Maryland from 16 April 2330-17 April 0030 UTC. During the ~30 min interval from 2330—2359 UTC, at least seven distinct mesovortices were detected in TDWR data (Figs. 3a-h). The mesovortices tended to form along the leading edge of the convective outflow boundary. The majority of these mesovortices were short-lived, lasting only a matter of a few minutes.

The detection of these mesovortices can be extremely challenging owing to their transience and small size. While they are more readily observed in TDWR data, many of the vortices may not be sampled at all by the WSR-88D radar owing to its comparably poorer temporal and spatial resolution. But even at one-minute temporal resolution, the vortices may appear as gate-to-gate velocity enhancements for as few as two scans before weakening, leading a warning forecaster to question whether they even are real features (e.g. vortex #1 in Fig. 3a-b).

The vortex centers generally have an often-swift eastward component to their motion in step with the overall movement of the convective line. As the vortices are shed from the leading edge of the outflow surge, they acquire a modest poleward component to their motion as well, leading to a scalloped trajectory. This scalloped shape also plays out in the observed concentrated damage swaths. Discontinuous, scalloped damage paths have been noted in many recent storm surveys of QLCS damage in the WFO LWX forecast area, suggesting that distinct vortices resulting from a cyclic vortexgenesis process are responsible for the damage. *In situ* observations on 16 April of leading-edge funnel clouds becoming wrapped in rain just prior to damage occurrence were conveyed during storm surveys by multiple sources.

d. Conceptual model

Atkins and St. Laurent (2009) suggest that QLCS mesovortices are most commonly generated as horizontal streamwise vorticity is tilted vertically (Fig. 4) along the leading edge of convective outflow beneath the updraft (which may be locally enhanced as localized outflow surges occur). However, local anecdotal observations (including the 17 April/0000 UTC KIAD RAOB) have shown that surface-based instability is not always present in QLCS tornado events. This observation suggests that convective updraft alone may not be solely responsible for vortex contraction via stretching. It is therefore speculated that upward motion (and thus vorticity stretching) may be enhanced along linear outflow also by accelerating air being lofted along localized outflow surges (Fig. 5).

Based upon the observed scalloped damage paths and circulation tracks, a vertical cross-section of vortexgenesis is shown in Fig. 6. Vortices form along the leading edge of repeated outflow surges, are shed poleward with time and are replaced with renewed vortices as cyclic outflow surges occur. In this way, scalloped, cyclic and discontinuous circulation tracks and damage paths are produced.

Analysis of WSR-88D data alone could lead to the concentrated tornadic damage paths being classified erroneously as a single tornado. But owing to their bottom-up development (e.g. Trapp et al. 1999) and coincidence with distinct mesovortices, the authors concluded that each such tornado is associated with a separate vortex in a manner analogous to supercellular cyclic tornadogenesis.

3. 27-28 APRIL 2011 TORNADOES

a. Synoptic overview

At 28 April 0000 UTC, a deep, closed upper low was located over Minnesota, while lead impulses on its southern and eastern periphery provided enhanced 500 hPa flow (Fig. 7, upper pane) over much of the southeastern and eastern United States. (One such wave was responsible for the historic tornado outbreak in Mississippi and Alabama during the afternoon and evening of 27 April.) At the surface (not shown), low pressure was centered over Michigan while a second closed surface low was located in western Indiana. A broad warm sector characterized by temperatures in the mid 70s and dewpoints in the upper 60s had spread northward through the entire Mid-Atlantic region owing to strong southerly low-level flow. The convective environment was characterized by modest instability and high shear (Fig. 7, lower pane). The hodograph was unidirectional through the lowest 700m and bore a general, orthogonally-oriented linear shape above. The low-level environmental vorticity vector was oriented toward the west-northwest. The shear was more than sufficient for organized updrafts.

Given the thermodynamic and dynamic fields, supercellular convection developed in the Piedmont region of Central Virginia in the afternoon of 27 April and moved through Southern Maryland during the evening. As mid-level flow increased, a low-level jet strengthened and lapse rates steepened overnight, more widespread cellular convection became common through the Shenandoah Valley. Convection again shifted eastward in the morning of 28 April as a slow-moving cold front crossed the region. Although the hodograph became less favorable synoptically for tornadoes during the morning (not shown), localized enhancements to the low-level shear supported brief tornadoes through mid-day before the threat waned.

b. Operational challenges of 27-28 April

Perhaps the greatest operational difficulty associated with the 27-28 April event was its sheer magnitude. Staffing levels were supplemented for a full 24 hours to accommodate warning operational needs, with at least one additional person dedicated exclusively to radar interrogation on each of three sequential shifts.

While KLWX radar was very helpful in diagnosing storm structure, its temporal scanning resolution often was inadequate to diagnose imminent tornadogenesis (Fig. 8). Frequent interrogation of TDWR data aided in this endeavor during the afternoon and morning phases of the tornadic outbreak, since these phases occurred in the geographic scope of the local TDWR network. During the overnight phase of the outbreak, however, this interrogation was hampered by the location of the storms in the Shenandoah Valley; out of range of the TDWR network. In some cases, KLWX inadequately sampled below 3.0km AGL.

During the overnight phase, it was especially difficult to distinguish tornadic from non-tornadic circulations. Many non-tornadic circulations exhibited signatures that looked at least as organized as their tornadic counterparts and yet did not produce a tornado (e.g. Fig. 9). Assessing differences between mesocyclones was complicated further by overnight storms' distance from the radar, and lack of visual reports of tornadoes due to darkness and/or the rural location of the parent circulations.

An additional challenge was encountered subsequent to warning operations, when numerous damage reports arrived at WFO LWX. A rapid transition from warning operations to data triage was undertaken to accommodate an increased flow of damage data. Additional staff were dedicated to processing damage reports, culling media sites for photo and video documentation of damage and directing survey teams.

The NSSL SHAVE project (Ortega et al. 2009) has demonstrated success in obtaining storm reports via targeted phone calls, and such methods also proved successful at WFO LWX. Targeted calls were made, and storm survey teams investigated, along radar-derived circulation tracks in locations where no damage had been reported. In many cases, severe weather events were obtained.

Storm damage surveys were undertaken as quickly as possible to document damage before it was cleaned or removed. Surveys continued through mid-May, however, given the number of required surveys and the size of the WFO LWX forecast area. Some damage was surveyed via novel means (e.g., via real-time, remotely-accessed cameras from a helicopter directed to fly along the path of radar-derived circulation tracks). Sporadic damage reports arrived at WFO LWX even months afterward, which highlights the scope and magnitude of this 24-hour tornado outbreak. A complete map of tornado track geography is shown in Fig. 10.

4. SUMMARY/CONCLUSIONS

Two significant tornado episodes occurred in April 2011 in the WFO LWX forecast area. Radar perspectives were presented (including dual-radar evaluation of supercell tornadogenesis), and some operational aspects of these two episodes were discussed. FAA Terminal Doppler Weather Radars proved invaluable to supplement, both temporally and spatially, the available WSR-88D radar data and to aid subsequent storm survey teams in isolating the geography of their damage searches.

A conceptual model of a QLCS non-mesocyclonic tornadogenesis process was offered in light of circulation tracks and damage path shape determined during QLCS storm events in the WFO LWX CWA. This model has been of great benefit to survey teams, who have occasionally found difficulty in fitting damage paths to a known conceptual model.

Of the challenges illuminated by the 27-28 April tornado outbreak, of great importance was the enhanced staffing required and implemented. The long duration of this unprecedented event required meteorologists dedicated solely to radar interrogation for nearly a full 24-hour period. The geographical scope of this event also highlighted the need to devote staff exclusively to the data organization role immediately after the event concluded to ensure timely surveys and thorough documentation of damage.

5. REFERENCES

Atkins, N.T. and M. St. Laurent, 2009: Bow Echo Mesovortices, Part II: Their Genesis. *Mon. Wea. Rev.* **137**, pp 1514-1532.

Ortega, K., T.M. Smith, K.L. Manross, A.G. Kolodziej, K.A. Scharfenberg, A. Witt and J.J. Gourley, 2009: The Severe Hazards Analysis and Verification Experiment. *Bull. Amer. Meteor. Soc.* **90**, pp 1519-1530.

Trapp, R. J., E. D. Mitchell, G. A. Tipton, D. W. Effertz, A. I. Watson, D. L. Andra Jr. and M. A. Magsig., 1999: Descending and nondescending tornadic vortex signatures detected by WSR-88Ds. *Wea. Forecasting,* **14**, 625–639.

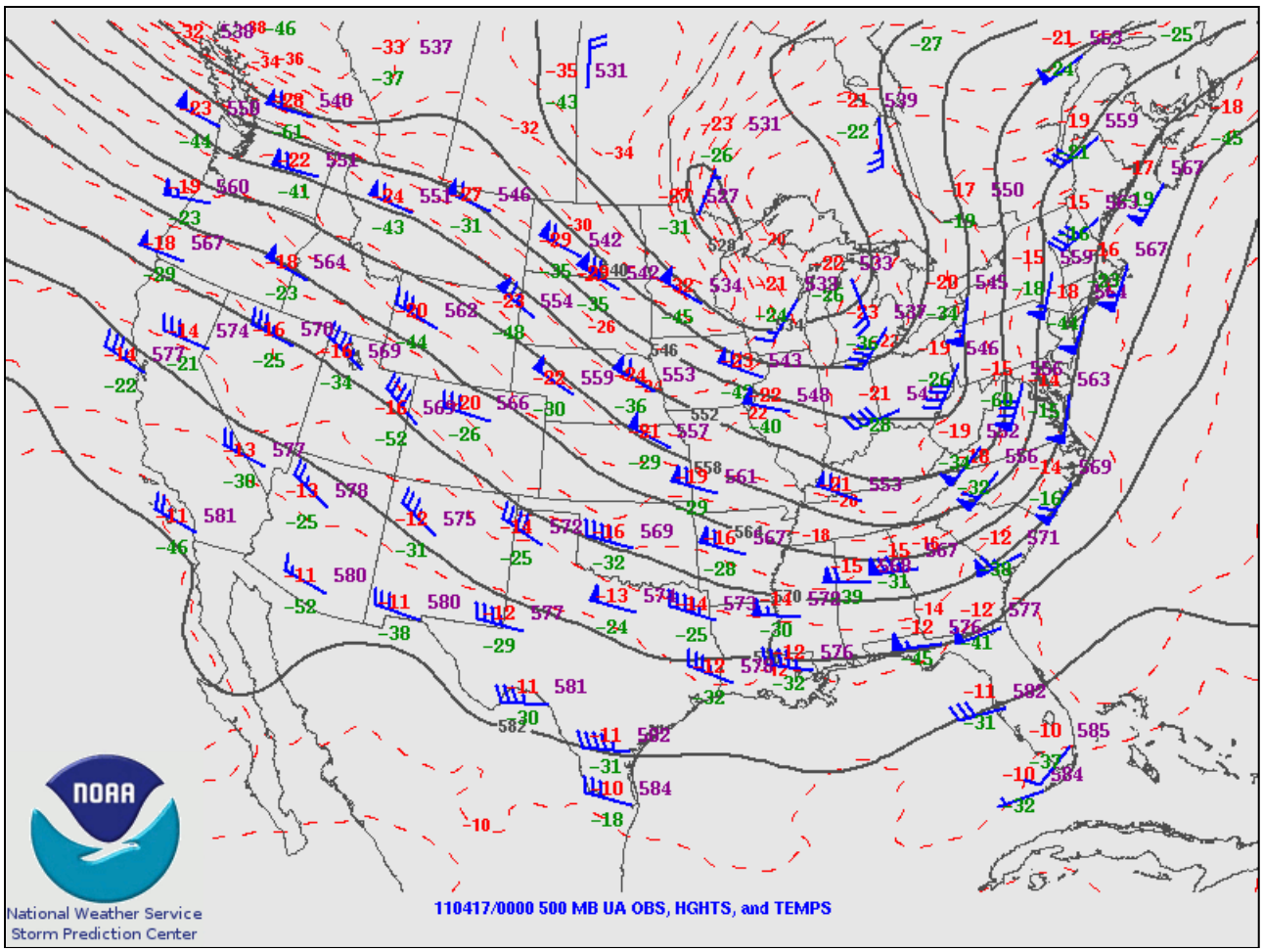

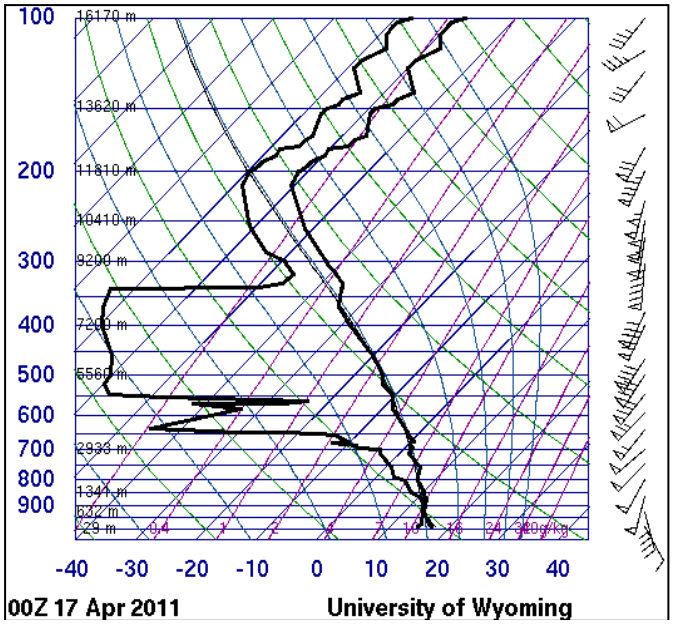

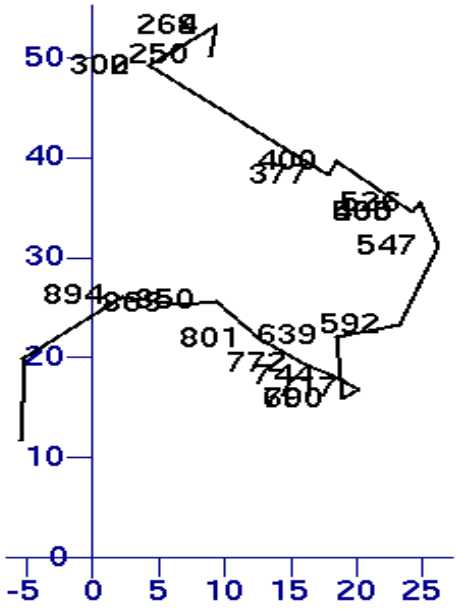

Fig. 1. Valid at 0000 UTC 17 April 2011, (top) A 500 hPa objective analysis from the Storm Prediction Center (SPC); (bottom) Observed KIAD RAOB and hodograph taken just ahead of an intense line of thunderstorms.

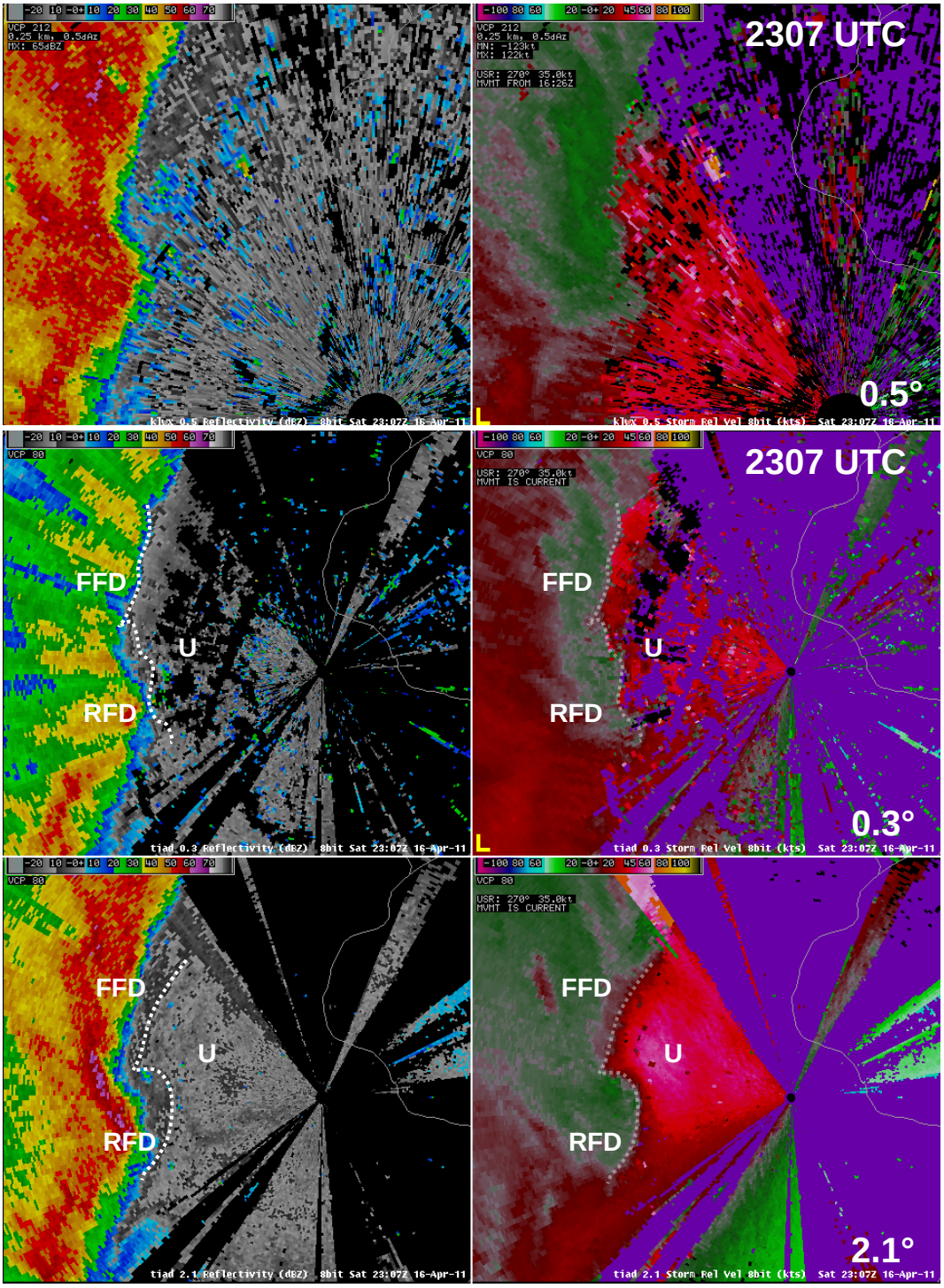

(2a)

Fig. 2. A comparison between (top pane) KLWX WSR-88D radar reflectivity and storm-relative velocity and (bottom panes) TIAD TDWR radar reflectivity and storm-relative velocity for a supercell thunderstorm near Leesburg, VA. Elevations and times are as indicated. KLWX data were not available in Fig. 2c owing to the lower temporal scanning resolution of the radar. In all figures, FFD represents the forward-flank downdraft, RFD represents the rear-flank downdraft and U represents updraft location. Hughesville, VA (the start of the tornado damage path) is denoted by a white X in Fig. 2b. Data shown are at (a) 2307 UTC, (b) 2310 UTC, (c) 2313 UTC, and (d) 2316 UTC.

(2b)

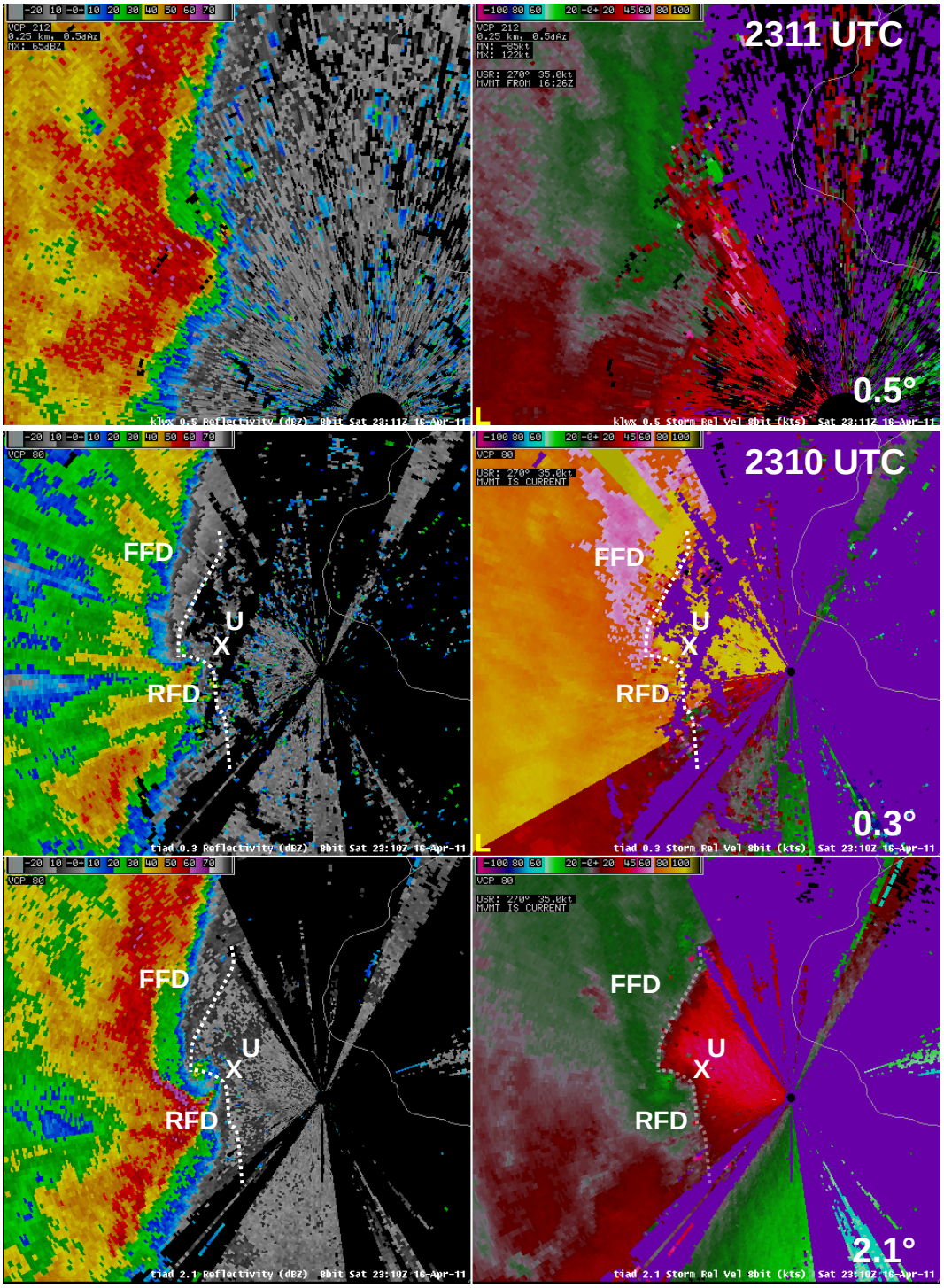

(2c)

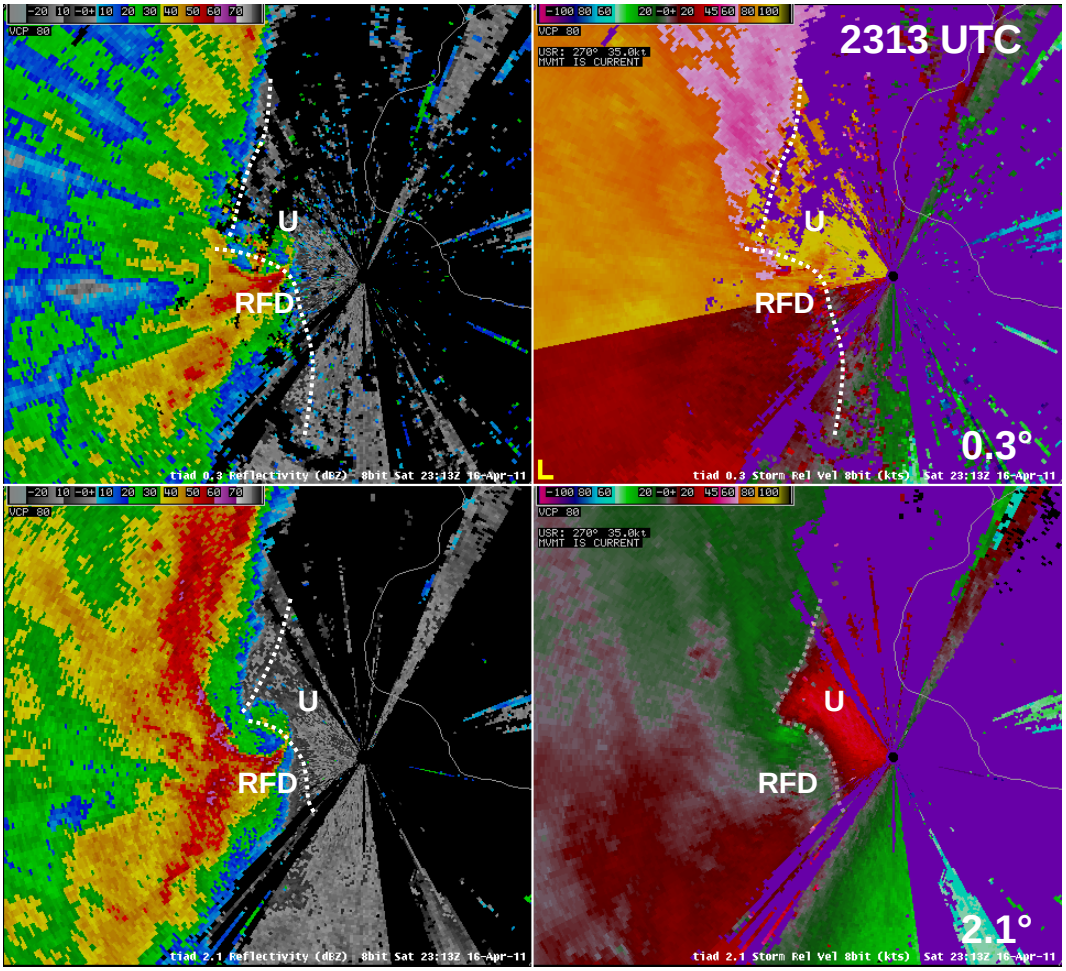
VCP 80
U
RFD
tiad 0.3 Reflectivity (dBZ) 8bit Sat 23:13Z 16-Apr-11
VCP 80
USR: 270° 35.0kt
MVMT IS CURRENT
2313 UTC
U
RFD
L
0.3°
tiad 0.3 Storm Rel Vel 8bit (kts) Sat 23:13Z 16-Apr-11
VCP 80
U
RFD
tiad 2.1 Reflectivity (dBZ) 8bit Sat 23:13Z 16-Apr-11
VCP 80
USR: 270° 35.0kt
MVMT IS CURRENT
U
RFD
2.1°
tiad 2.1 Storm Rel Vel 8bit (kts) Sat 23:13Z 16-Apr-11

(2d)

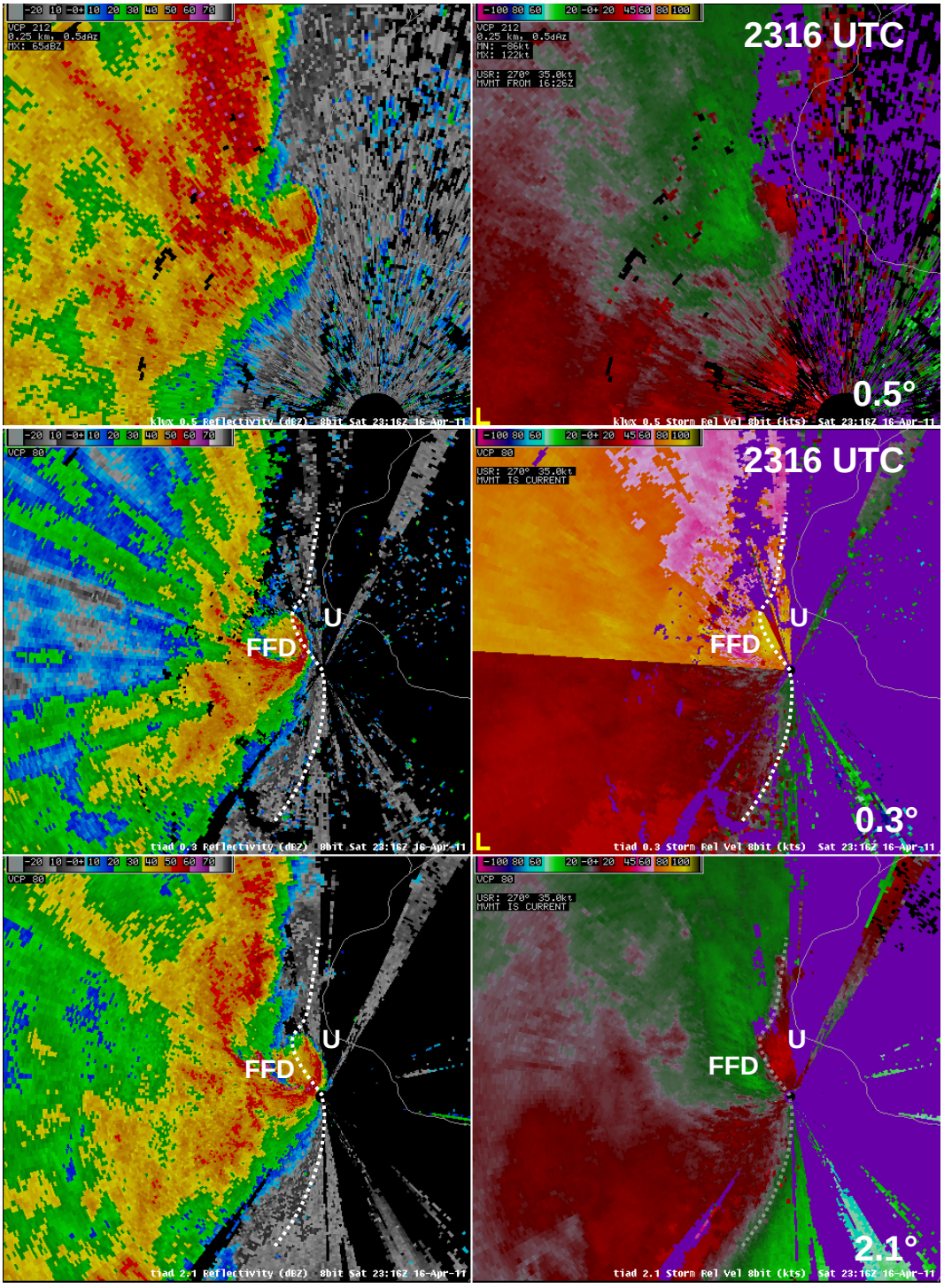

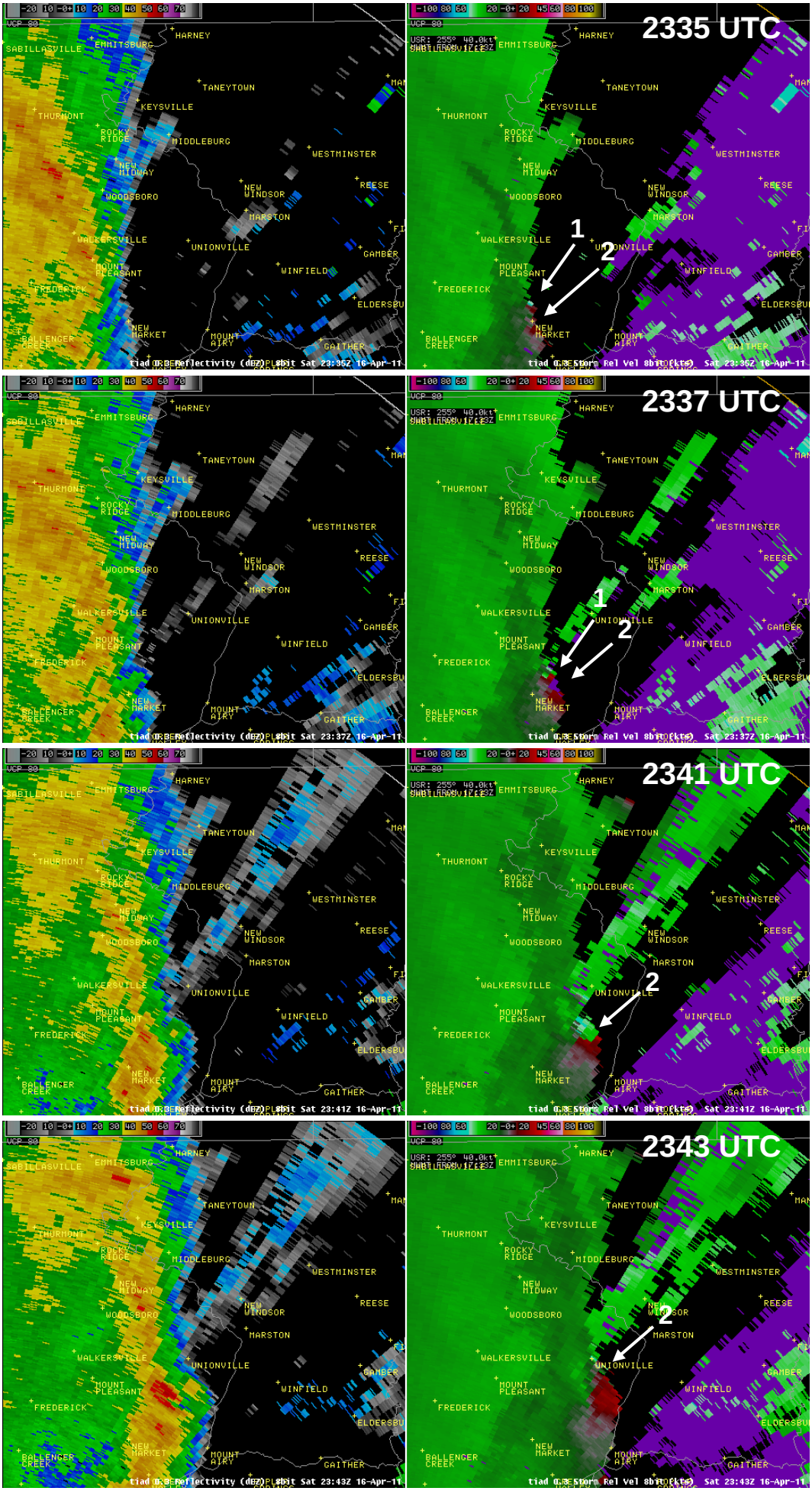

Fig. 3. Time sequence of 0.3° elevation radar reflectivity and storm-relative velocity from TIAD TDWR for a quasi-linear convective system in northern Maryland on 16 April 2011. Distinct mesovortices are identified by number for tracking purposes. Times shown are at (a) 2335 UTC, (b) 2337 UTC, (c) 2341 UTC, (d) 2343 UTC, (e) 2346 UTC, (f) 2350 UTC, (g) 2352 UTC, (h) 2356 UTC.

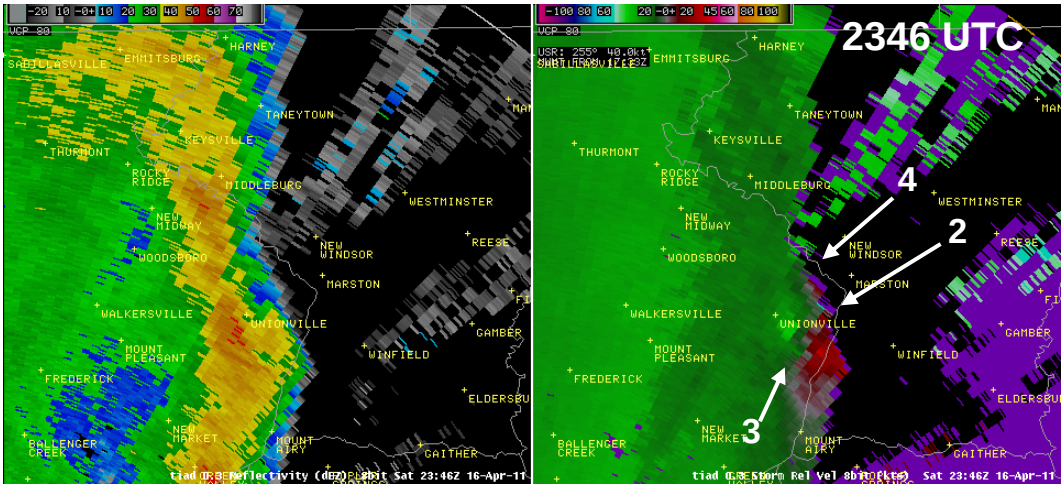
2346 UTC
4
2
3
tiad Q3E Reflectivity (dBZ) 8bit Sat 23:46Z 16-Apr-11
tiad Q3E Storm Rel Vel 8bit (kts) Sat 23:46Z 16-Apr-11

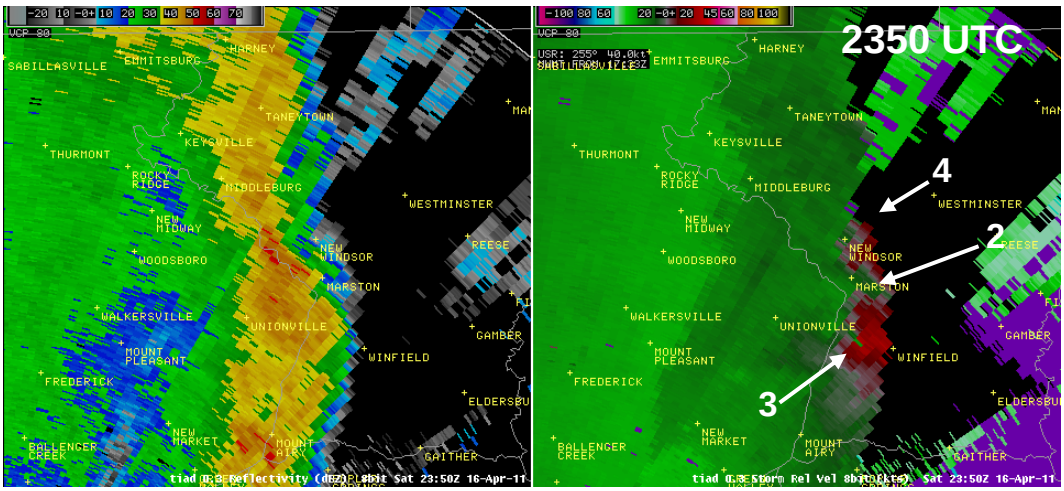
2350 UTC
4
2
3
tiad Q3E Reflectivity (dBZ) 8bit Sat 23:50Z 16-Apr-11
tiad Q3E Storm Rel Vel 8bit (kts) Sat 23:50Z 16-Apr-11

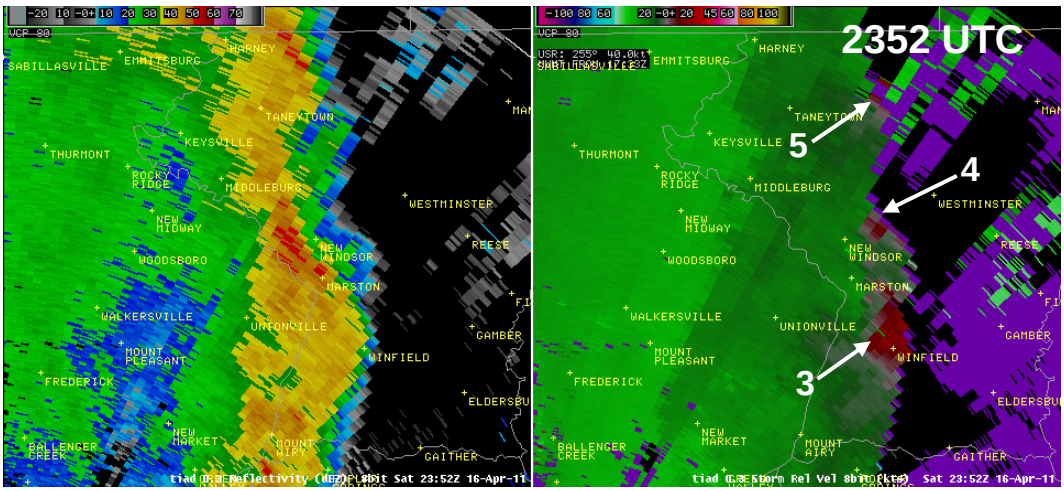
2352 UTC
5
4
3
tiad Q3E Reflectivity (dBZ) 8bit Sat 23:52Z 16-Apr-11
tiad Q3E Storm Rel Vel 8bit (kts) Sat 23:52Z 16-Apr-11

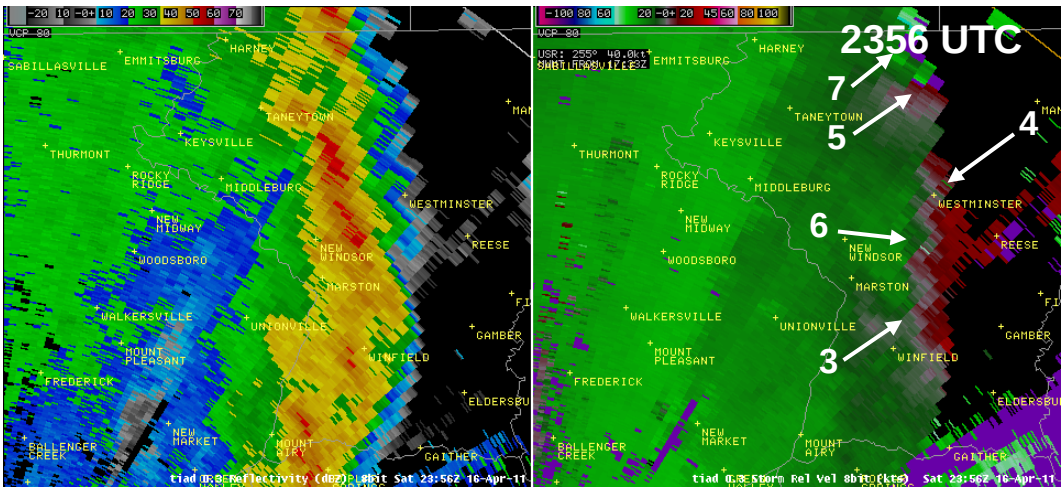
2356 UTC
7
5
4
6
3
tiad Q3E Reflectivity (dBZ) 8bit Sat 23:56Z 16-Apr-11
tiad Q3E Storm Rel Vel 8bit (kts) Sat 23:56Z 16-Apr-11

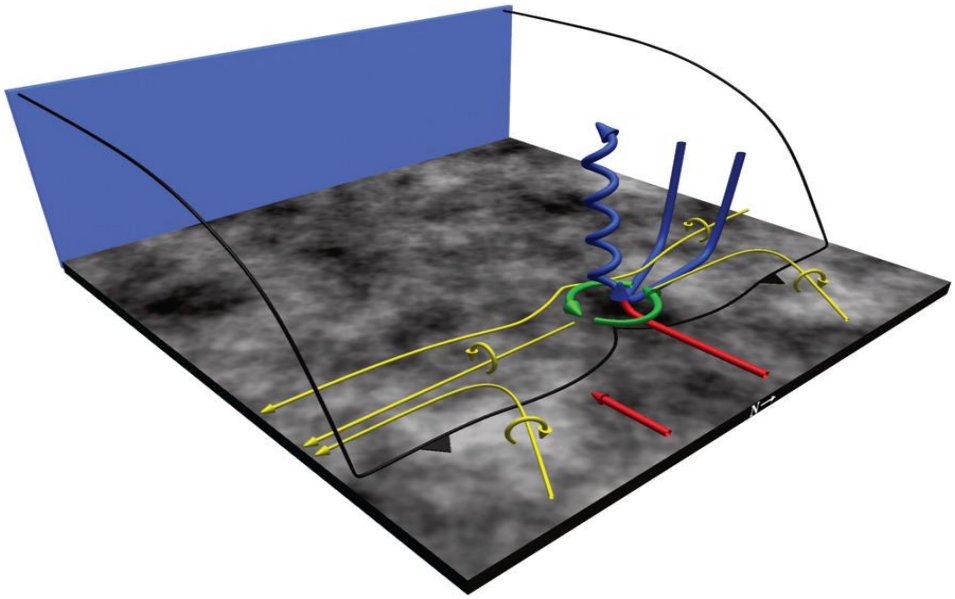

Fig. 4. Conceptual model of mesovortexgenesis in a quasi-linear convective system, from Atkins and St. Laurent (2009). Streamwise environmental vorticity and streamwise solenoidal vorticity from parcels in the descending outflow are tilted vertically along the leading edge of the convective outflow, resulting in a single cyclonic vortex.

Fig. 5. Especially in environments where surface-based instability is limited, vorticity stretching may be enhanced as air is lifted by localized outflow accelerations. Here, green arrows represent environmental vortex lines, dark arrows correspond to regions of enhanced vertical motion, and the blue arrow represents a surge in outflow. The surging outflow here provides enhanced lift and packs environmental vortex lines in much the same way as a rear-flank downdraft in supercell tornadogenesis.

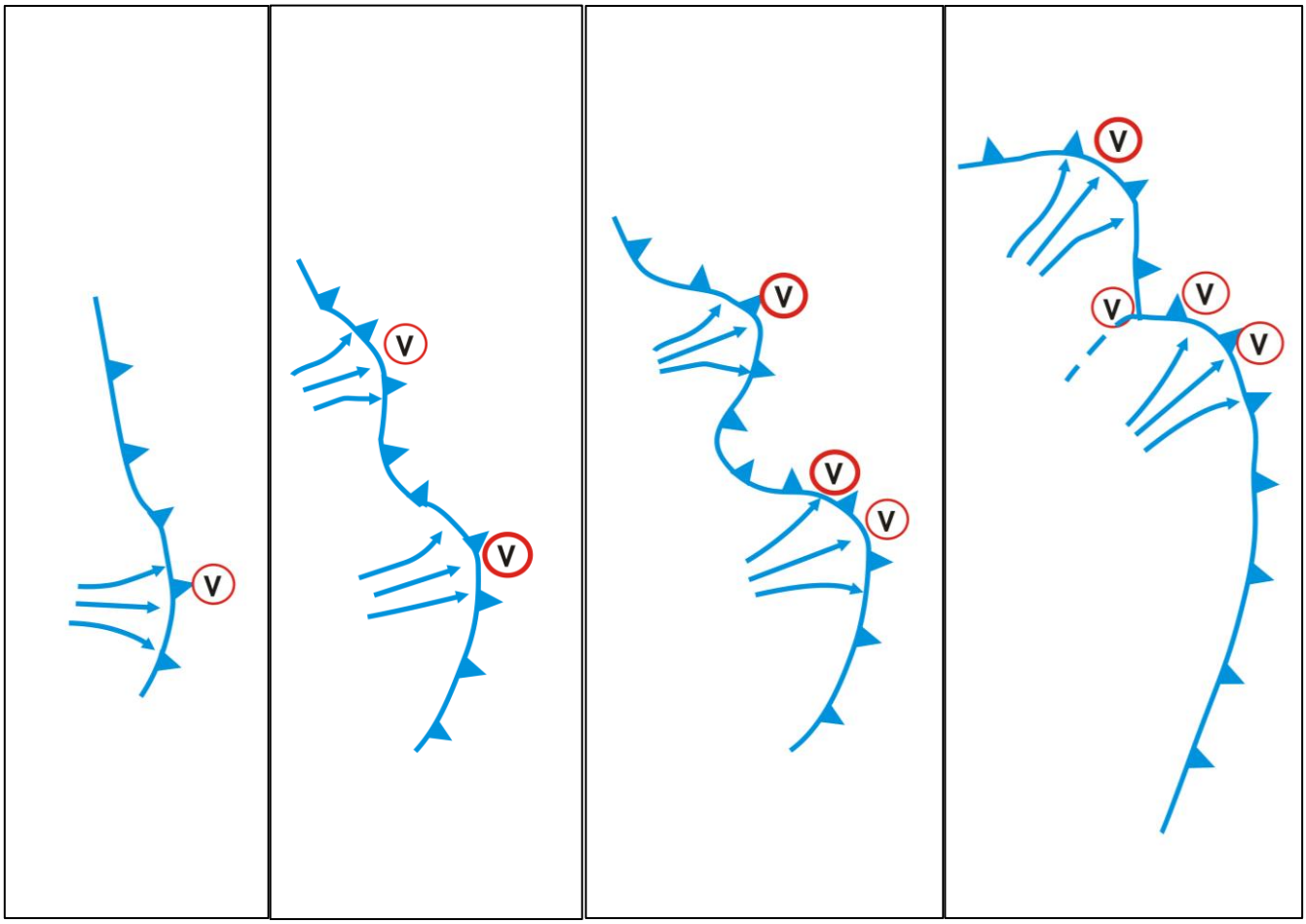

Fig. 6. A proposed conceptual model depicting the cyclic nature of mesovortex tornadogenesis as observed in TDWR data and damage surveys. Mesovortices are generated along the leading edge of outflow surges. These vortices are shed and replaced in a cyclic manner, leading to scalloped trajectories.

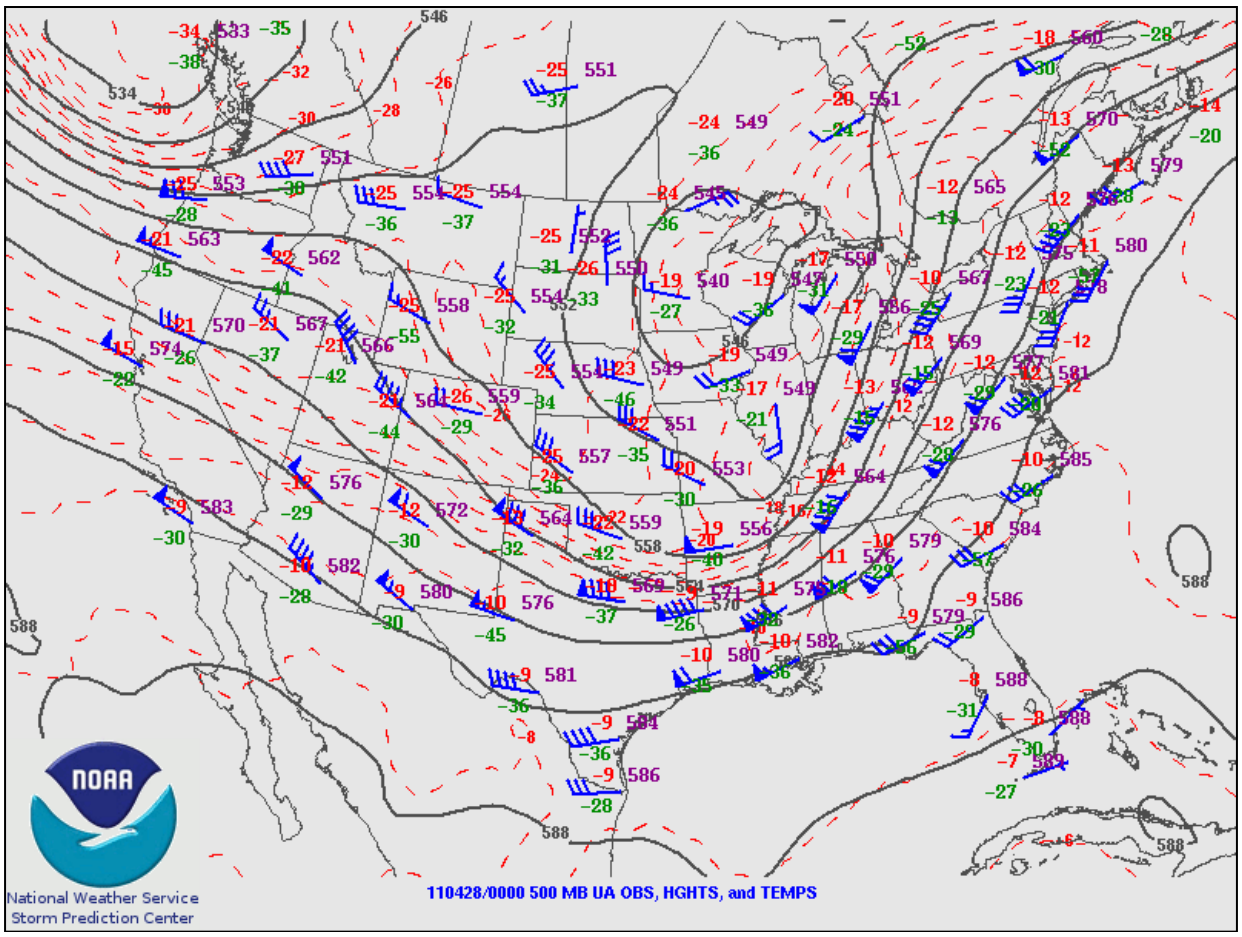

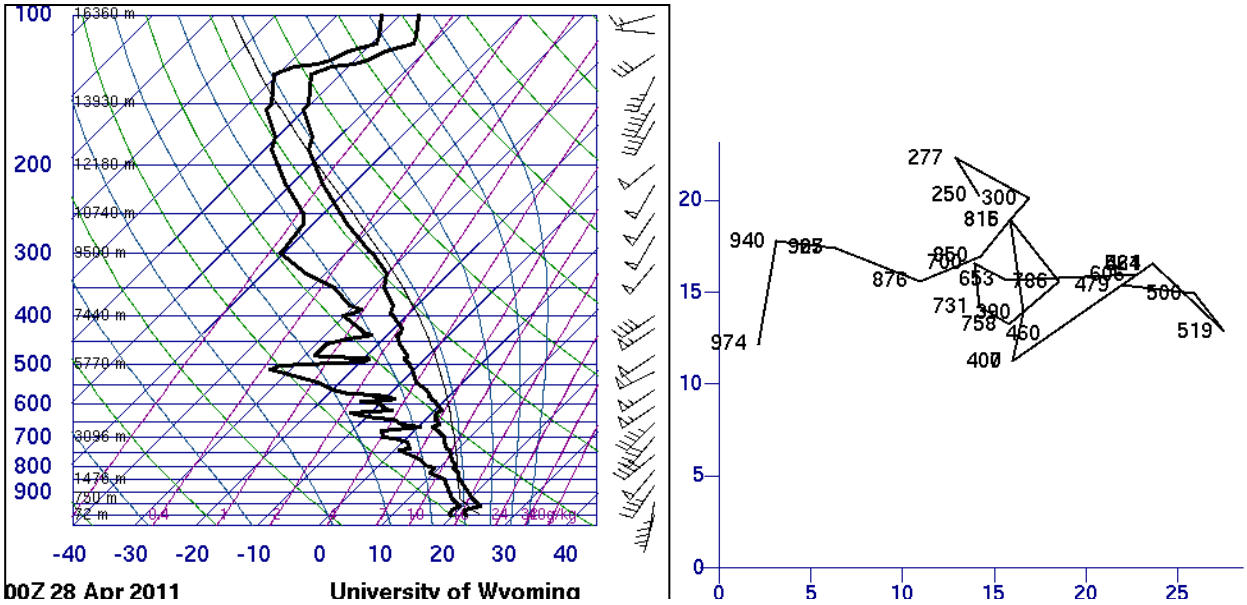

Fig. 7. Valid at 0000 UTC 27 April 2011, (top) A 500 hPa objective analysis from the Storm Prediction Center (SPC); (bottom) Observed KIAD RAOB and hodograph.

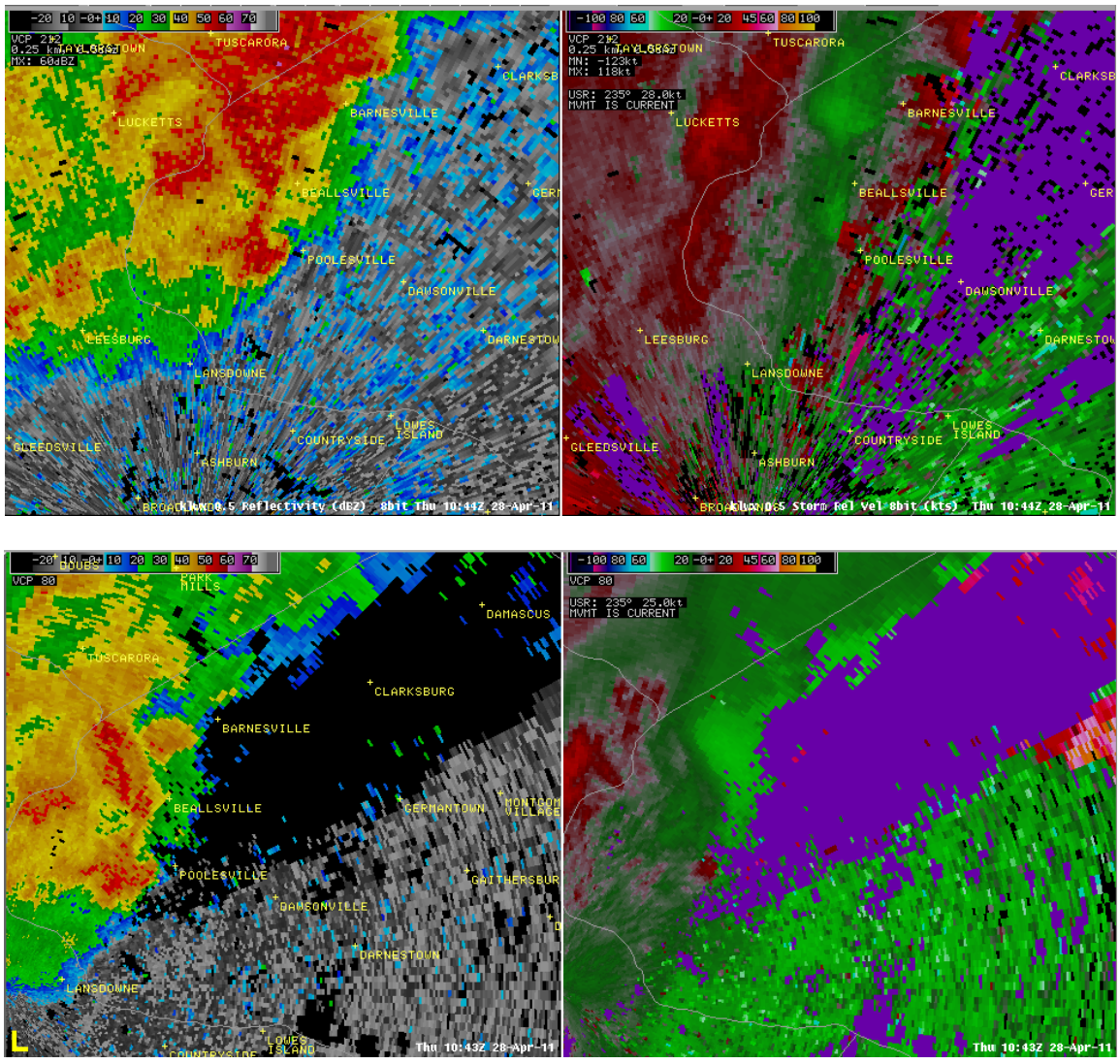

Fig. 8. Radar reflectivity and storm-relative velocity data for a storm in Montgomery County, MD at 1043-1044 UTC from (top) KLWX WSR-88D radar, and (bottom) TIAD TDWR. Owing to its higher temporal and spatial resolution, gate-to-gate shear of ~80 kt is detected in TIAD data that is not apparent in KLWX data. A brief and narrow EF-0 tornado occurred with this circulation, causing damage to fences and trees.

Fig. 9. Reflectivity and storm-relative velocity images from KLWX radar showing thunderstorms in the early morning hours of 28 April 2011. Each is an example of a non-tornadic storm that exhibited storm structure similar to or better than storms that produced tornadoes.

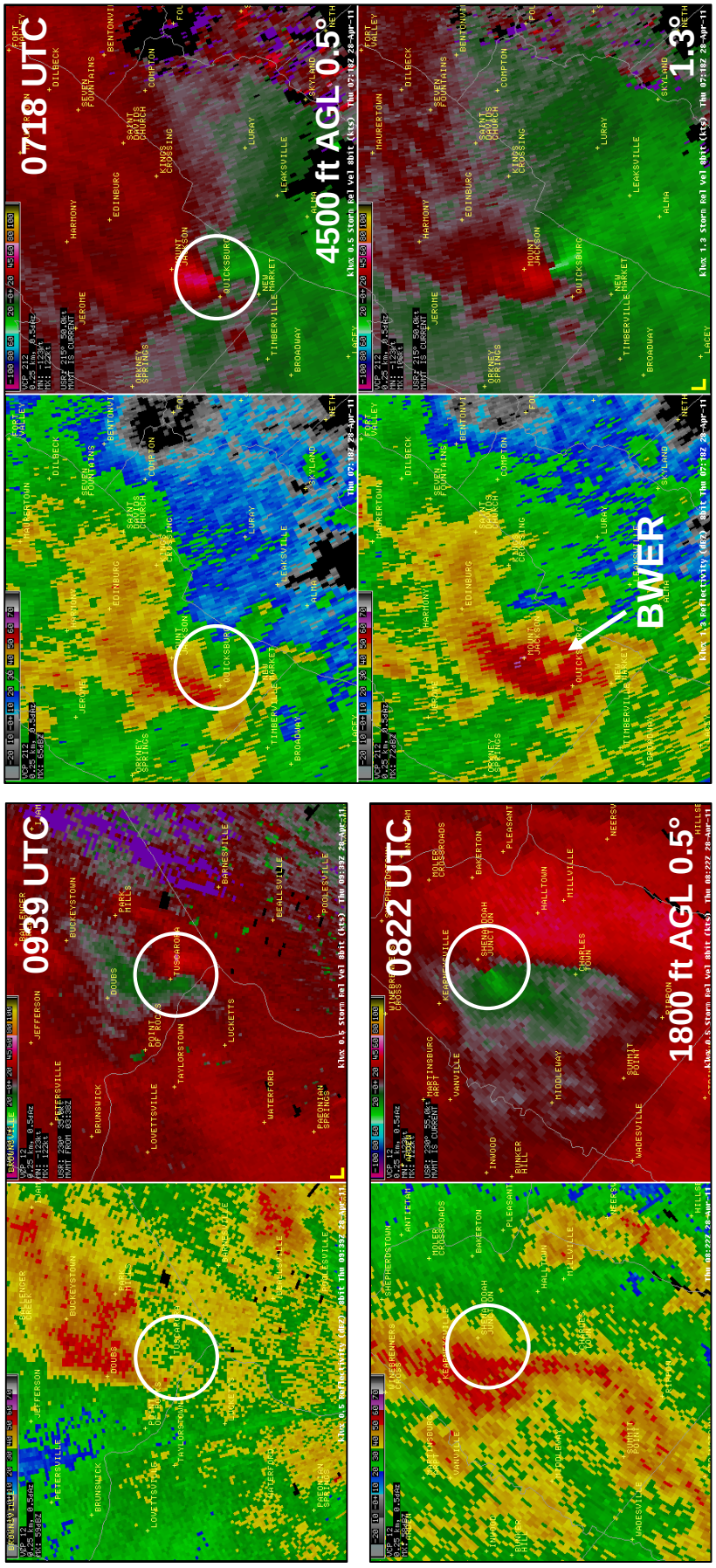

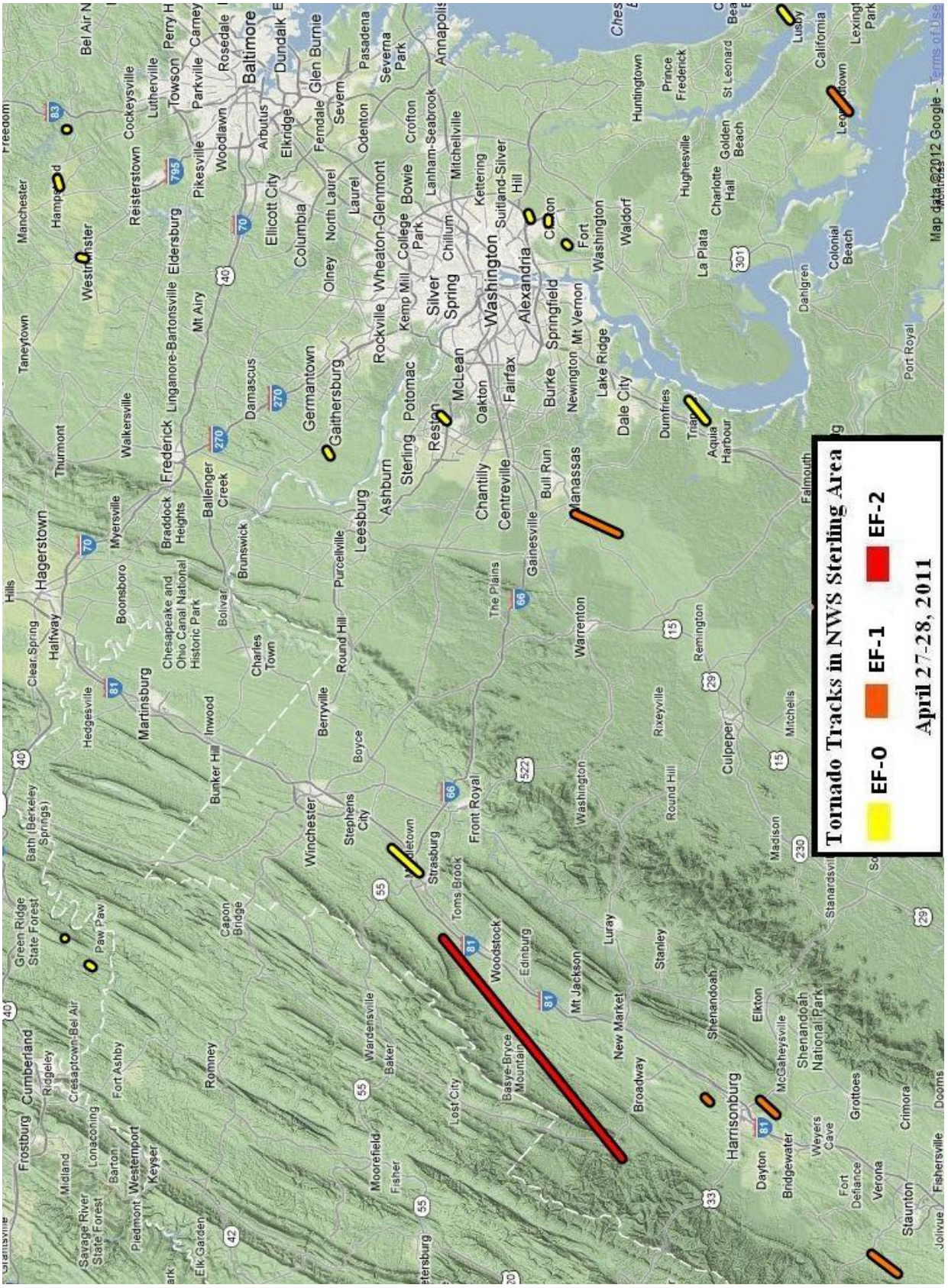

Fig. 10. Map depicting the tracks of the 19 tornadoes that occurred in the WFO LWX CWA during the 27-28 April outbreak. Tornadoes ranged from EF-0 to EF-2 in intensity.